NON-STEADY CHARACTERISTICS OF DISPERSION AND IGNITABILITY FOR HIGH-PRESSURIZED HYDROGEN JET DISCHARGED FROM A PINHOLE

Okabayashi, K.[1], Tagashira, K.[1], Kawazoe, K.[1], Takeno, K.[2], Asahara, M.[3], Hayashi, A.K.[4], and Komori, M.[5]

[1] Mitsubishi Heavy Industries, Ltd., Research and Innovation Center, 5-717-1 Fukahori, Nagasaki 851-0392 , Japan , kazuki_okabayashi@mhi.co.jp

[2] Toyota Technological Institute, Graduate School of Engineering, 2-12-1 Hisakata, Tempaku-ku, Nagoya468-8511, Japan, takeno@toyota-ti.ac.jp

[3] Gifu University, Facultyof Engineering, 1-1 Yanagido, Gifu 501-1193, Japan , asahara@gifu-u.ac.jp

[4] Aoyama Gakuin University, Graduate School of Science and Engineering, 5-10-1 Fuchinobe, Chuo-ku, Sagamihara-shi,Kanagawa 252-5258, Japan, hayashi@me.aoyama.ac.jp

[5] Japan Petroleum Energy Center, Sumitomo Fudosan Shiba-Koen Tower, 11-1, Shibakoen 2-Chome, Minato-Ku, Tokyo 105-0011, Japan, ma-komori@pecj.or.jp

ABSTRACT

Hydrogen gas concentrations and jet velocities were measured downstream by a high response speed flame ionization detector and PIV in order to investigate the characteristics of dispersion and ignitability for 40 to 82 MPa high-pressurized hydrogen jet which was discharged from the nozzle with 0.2mm diameter,. The lights emitted from both OH radical and water vapor species yielded from hydrogen combustion ignited by an electric spark were recorded by two high speed cameras. From the results, the empirical formula concerning the relations among time-averaged concentrations, concentration fluctuations and ignition probability were obtained to suggest that the relations would be expressed independent of hydrogen discharge pressure.

1.0 INTRODUCTION

Recently, hydrogen energy has been remarkably focusing as a clean energy in the future. There is a great expectation for fuel cell vehicles as one of utilizations of hydrogen energy. Therefore, to promote the introduction of fuel cell vehicles, the safe installation of hydrogen stations at urban areas is an urgent task. To do this, the relaxation of regulation for safety is necessary. In the present regulation, a distance between the dispenser of the station and public boundary is kept in more than a distance which is 1/4 lower flammable limit concentration distance (i.e. 1/4 LFL distance). For example of 82MPa filling station, the 1/4 LFL distance is about 8m and is too long to install the station at urban area that doesn't have any room, particularly in Japan.

It is not clarified whether the 1/4 LFL distance has any degree of risk or safety margin . Therefore, in order to examine the possibility to reduce the 1/4 LFL distance with a safe way, we investigate the characteristics of dispersion and ignitability on 40 to 82MPa high-pressurized hydrogen jet from a pinhole of 0.2mm diameter, where a leak from an aperture of piping joints etc. at a hydrogen station is thought as a typical accident case.

Although similar experimental research [1-3] have been performed these ten years, many studies have not been made under high pressures where real gas effect appears. Kouchi et al. [1] investigated the relation between concentration and ignitability of the choked hydrogen jet at the pressures of 40MPa and 20MPa with and without an obstacle in their jet. The characteristics of the upstream discharged hydrogen jet without choke was investigated by Schefer et al. [2] at the planar section along the jet axis . Ruggles et al. [3] studied the characteristics of a choked jet discharged from 1.5mm diameter with a 10:1 pressure ratio and demonstrated that the similarity law as the scalar field of no-choked jet could be applied to the choked jet by using an appropriate effective source exit diameter (equivalent diameter)

The purpose of this paper is to clarify that the dispersion and ignition characteristics of the hydrogen jet under very high pressures of 40 to 82MPa and to discuss the effect of different pressure on their characteristics.

2.0 EXPERIMENTAL SET-UP

High-pressurized hydrogen jet was discharged horizontally from a pinhole of 0.2mm diameter in the large enclosed space of the Hy-SEF facility, JARI (Japan Automobile Research Institute).

Two kinds of the experiment for the hydrogen jet; dispersion and ignition , were carried out. First of all, concentration and velocity on vertical plane including jet axis were measured downward by FID (Flame Ionization Detector) and PIV (Particle Image Velocimetry) system. They are called the dispersion experiment.

 Secondly, the gas on the jet axis was ignited by the electric spark and then the optical radiation emitted from both OH radical and water vapor (H_2O) species yielding from the ignited gas were recorded by two high speed cameras. The concentration of hydrogen was directly measured by Raman scattering system to record OH profiles by a high speed camera [4]. The shadowgraph image was also taken around the spark ignition point to visualize the ignited flame structure and to record by another high speed camera. These measurements were made simultaneously.

The schematic diagram of the measurement system for the ignition experiment is shown in Fig. 1.
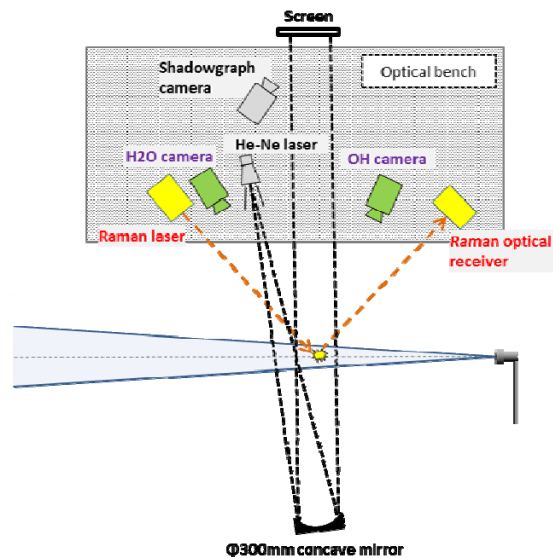

Figure 1. Outline of experiment measurement

2.1 Dispersion Experiment

In the dispersion experiment, the hydrogen gas containing a small amount of methane as the tracer was spouted into air. The concentration of methane in the jet was measured by the high-response speed flame ionization detector HFR500 (Cambustion Ltd.), where the gas in the jet is sampled through a syringe of 0.25mm inner diameter at the sampling rate of 200Hz and then the concentration of hydrogen is obtained from the concentration of methane, as follows.

$$C_{H_2} = C_{CH_4} / C_0 ,\qquad\qquad\qquad (1)$$

where C_0 is the concentration of methane at the exit of pinhole and C_{CH4} the concentration of methane measured by FID and C_{H2} concentration of hydrogen.

The velocities on the four vertical planes along the jet axis, where the centers of the planes were located at 0.5m, 1.0m, 1.5m and 2.0m from the nozzle (pinhole) exit, were measured by the two dimensional PIV system with a double pulse laser. The image of the area that is about 300mm

downstream and about 260mm high, where the center of the area coincides with that of the above-mentioned vertical plane, was taken at 15 Hz. The seeding of dioctyl sebacate (DOS) was fed immediately after the exit of the pinhole.

The dispersion experiment was carried out for 60MPa and 82MPa hydrogen jet. But PIV measurement wasn't made for 60MPa hydrogen jet because the flow field of 60MPa would be able to be estimated by the similarity with 82MPa.

2.2 Ignition Experiment

The ignition experiment was carried out only for 82MPa hydrogen jet. The electric spark with 3.5mm distance between two electrodes was installed on the jet axis and ignited the spouted hydrogen jet, which was 100% concentration of hydrogen without methane. The electric spark with 30mJ was generated at 10Hz during the discharge of hydrogen. But the spark occurred sometimes irregularly and occasionally because the generation of the spark depended on the state of flow between electrodes. The concentration of hydrogen at the ignited point was simultaneously measured by Raman scattering method (measured with 416.6nm wavelength) to be compared with the FID's results, so that we could check whether the difference inmeasurement method influences the measured concentration or not. Also, the optical radiations from both OH radical and water vapor (H_2O) species ignited by the electric spark and emitted from hydrogen jet were detected and recorded at 500fps by two high speed cameras to measure their concentrations. The two high speed cameras of FASTCAM SA-X2 (Photron Ltd.) and PHANTOM V2551 (Nobby Tech. Ltd.) were used for OH radical and H_2O, respectively. The emitted light from OH radical was amplified by the image intensifier C10880-03 (Hamamatsu Photonics) and then recorded through the band pass filter (299 to 318nm), where the incident light into the camera for OH radical was blocked during the spark because the image intensifier could be damaged by a high-intensity spark. The emitted light from H_2O was recorded through the long pass filter (cut wave length 830nm) during the measurement. Furthermore, the visualization of flame ignited by the spark was recorded by the shadowgraph imaging system using a He-Ne laser with 632.8nm wavelength to avoid the interference with Raman scattering lights and emitted lights from OH radical and H_2O.

In the ignition experiment, four kinds of measurements such as concentrations of hydrogen, OH radical, water vapor and the visualization of flame were performed simultaneously. The outline of the experiment is shown in Fig. 1.

The spark generation was judged by the H_2O images captured through a camera, except that the image of OH radical wasn't recorded while the 10Hz spark was used.

The ignition experiment was carried out only for 82MPa hydrogen jets when the location of the spark was moved every 0.1m from 0.4m to 2.0m downstream from the pinhole exit.

2.3 40MPa Hydrogen Jet Experiment

40MPa hydrogen jet experiments [1] similar to the 82MPa dispersion and ignition experiments were also carried out in order to discuss the effect of different pressure from 82MPa on the ignitability of hydrogen jet. Since the 40MPa experiment was carried out at outside, unlike the 82MPa experiment, their results were influenced somewhat by the wind and were performed at low wind conditions (almost calm). In the 40MPa experiment, the hydrogen concentration and the velocity of the jet were measured by FID and PIV system in the similar way as the 82MPa experiment, respectively. The images of OH radical was also taken and recorded by the high speed camera of FASTCAM-APX (Photron Ltd.) with the band pass filter (303 to 323nm) through an image intensifier. The major differences of the 40MPa experimental condition from 82MPa experiment were that the electric spark energy is 120mJ and the distance between electrodes is 1.5mm. The effect of the above-mentioned differences on the experimental results seems negligible comparing with a changeable outdoor wind.

3.0 EXPERIMENTAL RESULTS

3.1 Velocity Measurement Results

The streamwise velocity U in the spouted jet of 82MPa was measured by the PIV system at the 4 representative locations along the jet axis. From these results, the velocity U and its half width b_u were analyzed as shown in Fig. 2(a) and (b), then the velocity U on the jet axis can be expressed by Equation (2) using the after-mentioned equivalent diameter θ. The half width b_u is expressed as a function of the distance X from the exit by Equation (3).

$$U = 7600/(X/\theta) \tag{2}$$

$$b_u = 0.091X \tag{3}$$

$$\theta = D \cdot (\rho_e / \rho_a)^{0.5}, \tag{4}$$

where D is the diameter of a pinhole (the exit of the jet), ρ_e density of hydrogen at the exit and ρ_a density of air. The ρ_e is the density at the choke condition which is obtained under an isotropic change of ideal gas.

These expressions are consistent with the previous studies at choke conditions [3, 5] and no choke conditions [6]. Particularly, the expression of the half width b_u is in common whether the choking occurs or not .

(a) Streamwise velocity   (b) Half width of stramwise velocity
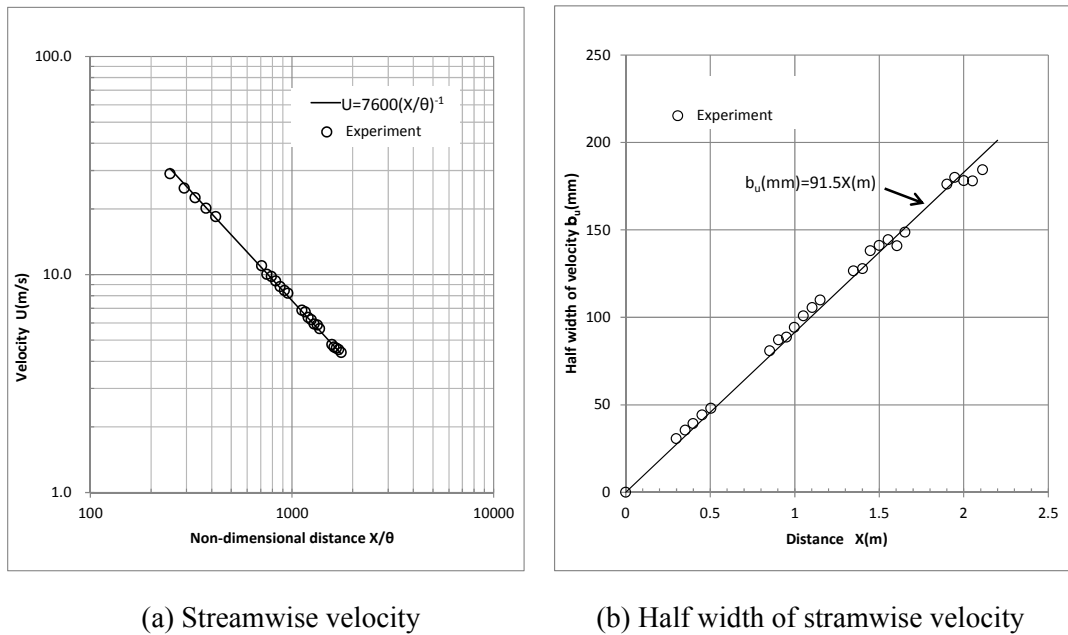
Figure 2. Results by PIV measurement

3.2 Concentration Measurement Results

In this section, the results of hydrogen concentration measured by FID in the dispersion experiment are summarized. The time dependent concentration data were analyzed using the following statistic quantities: the time averaged concentration C, the half width of the concentration b_c, the intensity of concentration fluctuations σ_c/C, the occurrence probability of concentration P and the spectrum of concentration S. The time averaged concentration C and the occurrence probability of concentration P

4

were also compared with the data from Raman scattering measurement in the ignition experiment to check whether the difference in the concentration measuring method influences the experimental results.

The concentration distribution along the jet axis is shown in Fig. 3. The concentrations of 82MPa, 60MPa and 40MPa measured by FID and 82MPa by Raman scattering method are shown in Fig. 3. All data are almost in agreement except for the data in the nearfield by Raman. In the near jet exit, hydrogen is ignited due to the existence of flammable mixture where hydrogen concentration measured by Raman decreases than the one by FID. Moreover, there is a possibility that the measuring point is a slight out of alignment on the jet axis in the near jet exit.

From the results, it is concluded that the difference in the measuring methods of concentration doesn't influence the experimental results and hydrogen concentration measured by FID is appropriate.

The distance X from the exit of the jet in the horizontal axis in Fig. 3 is non-dimensional by the equivalent diameter θ defined by Equation (4).

It is found in Fig. 3 that the concentration downstream along the jet axis decreases in inverse proportion to the distance similarly to the previous studies [3, 5, 6, 7, 8, 9]. In this study, the concentration profile along the jet axis was expressed by the following Equation (5).

$$C = 4300 \cdot \left(X / \theta \right)^{-1} \qquad (5)$$

The results imply that the region downstream along the jet axis up to the LFL distance (the distance downstream the exit of the jet to decrease to LFL concentration (4%), is influenced by momentum more strongly than by buoyancy.

The half width b_c of concentration is obtained from both vertical and horizontal profiles of concentration as shown in Fig. 4. It is found by approximating the experimental data of a Gaussian distribution using the method of least squares. It contains relatively large errors because the sufficient amount of data were not obtained. Particularly, b_c with a parenthesis notation in Fig. 4 is incredible because of the approximation by only three measuring points.

Figure 3. Concentration Distribution along Jet Axis

Except for the data of three points approximation, the half width b_c could be expressed by the following Equation (6). It is almost the same results as the previous studies for both a compressible jet with choke conditions [3] and an incompressible jet without choke conditions [6, 10].

$$b_c = (0.10 \sim 0.11) X \qquad (6)$$

The intensities of concentration fluctuations at 82MPa and 60MPa are shown in Fig. 5. The distance from the jet exit is normalized by the equivalent diameter θ defined by Equation (4). The vertical axis σ_c/C is expressed by Equation (7). The intensity of concentration fluctuations, σ_c/C, is almost constant downstream the jet which is similar to the previous studies [3].
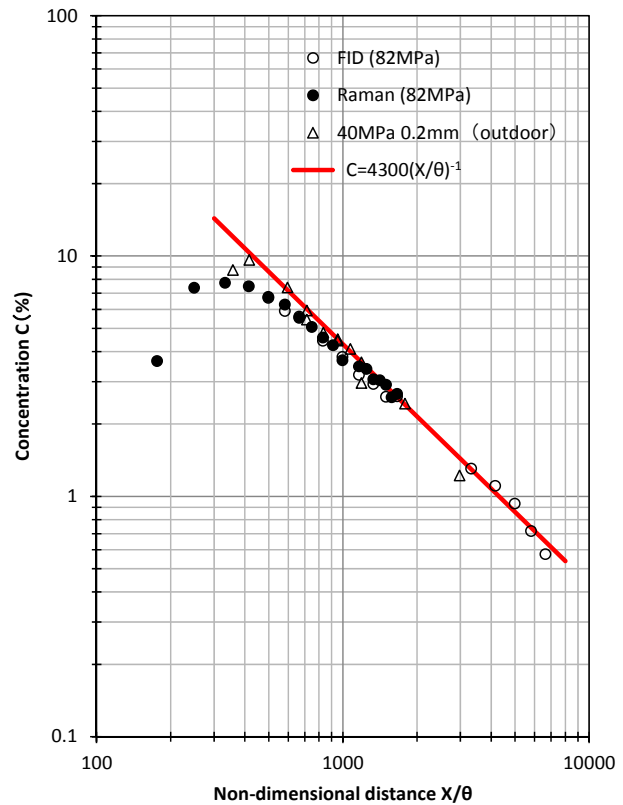
$$\sigma_c / C = 0.20 \sim 0.25 ,\tag{7}$$

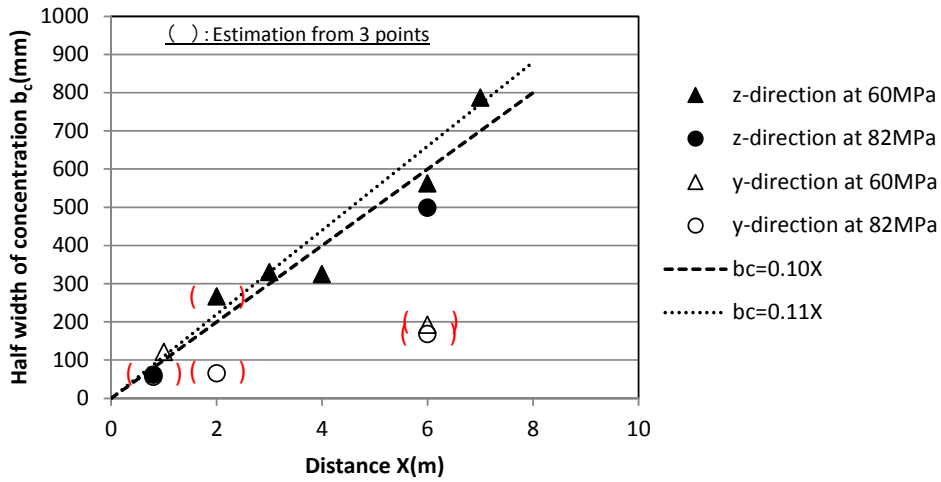where σ_c is a standard deviation of concentration fluctuations.

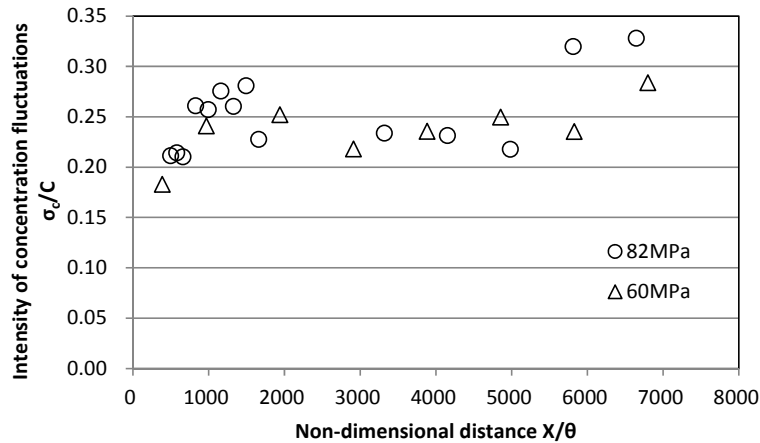Figure 4. Half Width of Concentration

Figure 5. Intensity of Concentration Fluctuation

We also examined two characteristics of concentration fluctuation in addition to the standard deviation. One is the occurrence probability distribution of concentration along the jet axis, P_c, and another is the power spectrum of concentration, $f \cdot S/\sigma_c^2$.

The occurrence probability distributions measured at X=0.6m and 2.0m on the 82MPa jet axis are shown in Fig. 6. The probability distribution functions P's approximated by Log-normal and Gaussian distributions, which are expressed by Equations (8) and (9), respectively, were also indicated in Fig. 6. The values C and σ_c/C in Equations (8) and (9) were obtained directly from the stochastic analysis of concentration data measured in the experiment. It was found that Gaussian distribution fits experimental data better than Lognormal distribution because of the measurement on the jet axis. In the past studies for passive plume [11, 12], it was examined whether various probability distribution functions would fit the stochastic characteristics of concentration fluctuations measured in the field or laboratory experiments. As a result, it was pointed out that the probability distribution of concentration

6

was non-Gaussian distribution [11]. But in the present study, the Gaussian distribution fits the measurement results the same as the previous studies [1, 2]. This cause is probably that the measurement is not conducted for a passive plume, but done for a very strong jet and on its jet axis

$$P(c) = \frac{1}{\sqrt{2\pi}\sigma \cdot c} Exp\left(\frac{(\ln c - m)^2}{2\sigma^2}\right) \qquad \text{, for Log-normal distribution} \tag{8}$$

$$\sigma^2 = \ln\left((\sigma_c/C)^2 + 1\right), \; m = \ln\left(C/\sqrt{1 + (\sigma_c/C)^2}\right)$$

$$P(c) = \frac{1}{\sqrt{2\pi}\sigma_c} Exp\left(\frac{(c - C)^2}{2\sigma_c^2}\right) \qquad \text{, for Gaussian distribution} \tag{9}$$

where C is the averaged concentration, c the instantaneous concentration and σ_c/C the intensity of concentration fluctuations. The values C and σ_c/C are also obtained from Equations (5) and (7), respectively.
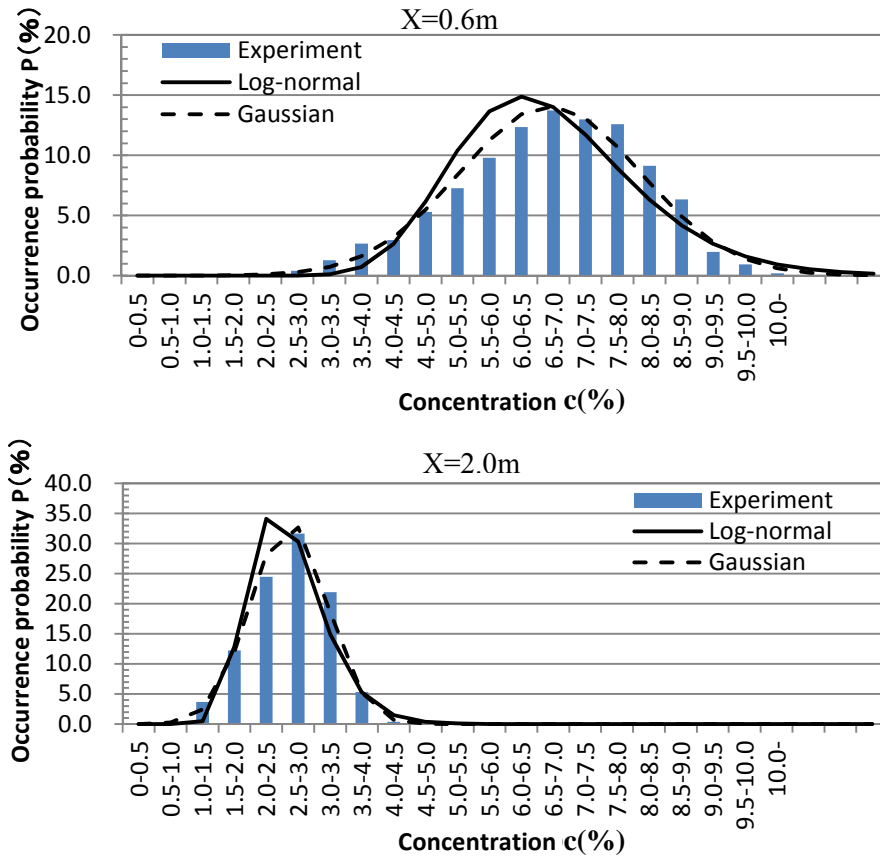
Figure 6. Occurrence Probability Distribution of Concentration on Jet Axis at 82MPa

In addition, the occurrence probability of flammable concentration P_c (4 to 75%) along the jet axis is summarized in Fig. 7. The relation between the flammable concentration probability P_c and the non-dimensional distamce X/θ shown in Fig. 7 can be also obtained by Equations (8) or (9) because Equations (8) and (9) are in a good agreement with the experiment data.
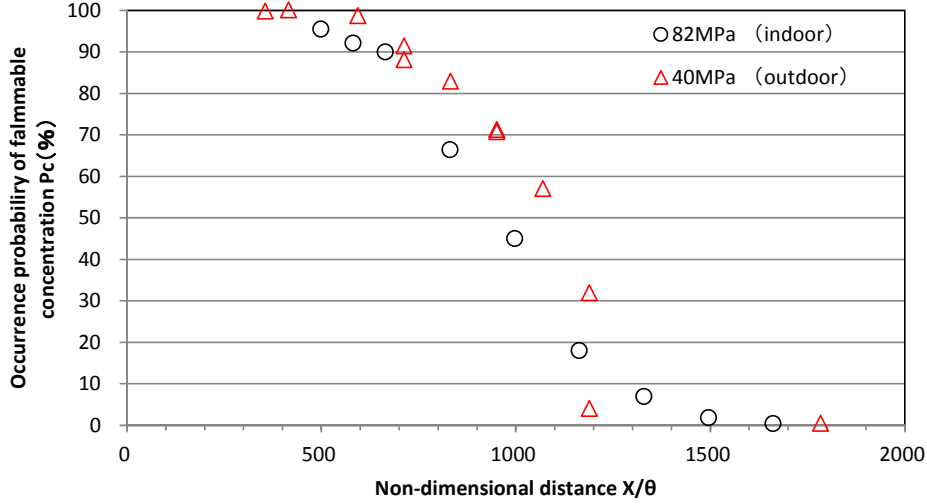
Figure 7. Occurrence Probability of Flammable Concentration

Another characteristics is the power spectra of concentration at 82MPa and 60MPa as shown in Fig. 8, where the power spectrum S is normalized by the frequency f and the standard deviation of concentration σ_c. The frequency f is also normalized by the streamwise flow speed U on the jet axis and the half width of concentration b_c is in the similar way as Hanna [13]. The flow speed U and the half width of concentration b_c are obtained by Equations (2) and (6), respectively. Fig. 8 is indicated in non-dimensional notation in addition to the overbar. The non-dimensional spectra of 82MP and 60MPa are in a good agreement each other. It is considered this is why the self-preserving jet is satisfied up to the LFL distance. It is noted the representative speed U of 60MPa in Equation (10) is obtained from the above-mentioned Equation (2) because of no measurement of velocity in the 60MPa experiment. It is assumed Equation (2) is satisfied even at 60MPa.

The spectrum distributions of 82MPa and 60MPa could be approximated by Equation (10) proposed by Pasquill and Bulter [14] and then Equation (10) is indicated by a solid line in Fig. 8.

$$\overline{S} = \frac{A \cdot \overline{f} / \overline{f_m}}{(1 + 1.5 \cdot \overline{f} / \overline{f_m})^{5/3}} \quad (A = 1.3, \ \overline{f_m} = 0.35) \tag{10}$$

$$\overline{S} = f \cdot S / \sigma_c^{\ 2}, \quad \overline{f} = f \cdot b_c / U \ ,$$

where $\overline{S}$, $\overline{f}$ and $\overline{f_m}$ are non-dimensional quantities of a spectrum, a frequency and a frequency of spectrum peak, respectively. In addition, the values of A and $\overline{f_m}$ are determined to fit the spectrum distribution measured in this experiment.

This means the property of concentration fluctuations does not change depending on pressures and locations along the jet axis by some adequate scaling.
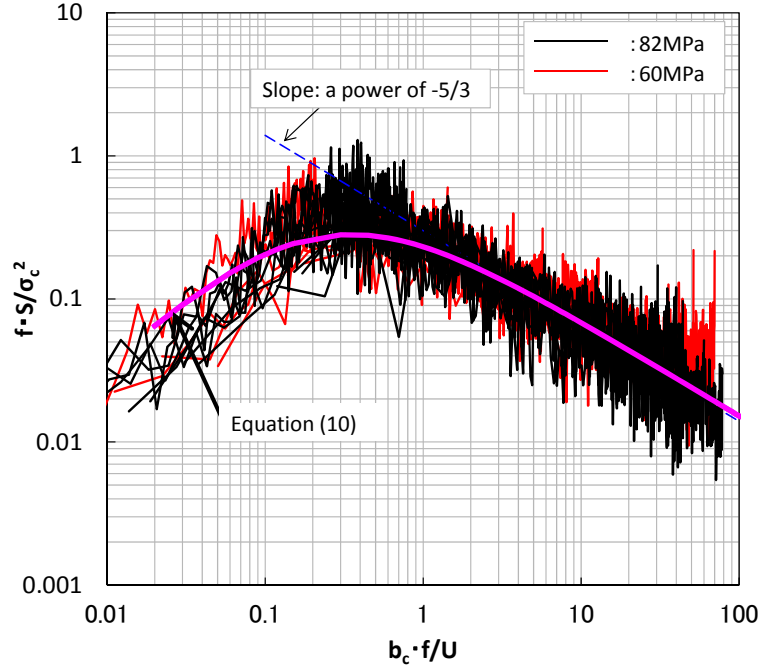
Figure 8. Spectrum of Concentration at 82MPa and 60MPa

3.3 Ignition Probability

In the ignition experiment, three high speed cameras were used for the imaging of the lights emitted from OH radical, H_2O and shadowgraph of the flame, respectively. The example of the recorded images is shown in Fig. 9. There were the sparks generated irregularly apart from 10Hz. Therefore, the condition of the spark generation was judged by whether the spark was captured by the high speed camera for H_2O. From this examination, the number of the total ignition was obtained.

The ignition experiment was carried out during 20 to 30 seconds for each measurement. Therefore, the number of total ignition are about 200 to 300 under one experimental condition because the most sparks were generated at the interval of 0.1 seconds (10Hz). The ignition probability P_f is defined by the following Equation (11):

$$P_f = Ni / Ns, \tag{11}$$

where Ni is the total number of ignited trials and Ns the total number of spark generations in a measurement, and then ignitions were determined by whether the light emitted form OH radical was detected.

The ignition probability P_f against the distance from the exit of the jet is shown in Fig. 10. It is found that the ignition probabilities of 82MPa and 40MPa decreases in the similar way each other as the location of the spark moves away from the exit of the jet. This could be expected by the similarity of concentration, concentration fluctuations and occurrence probability of flammable concentration with respect to X/θ, as shown in Fig. 3, Fig. 5 and Fig. 7 (i.e. Equation (8) or (9)), respectively. Moreover, it would be also attributed to the self-similarity of the power spectrum of concentration fluctuation as shown in Fig. 8.
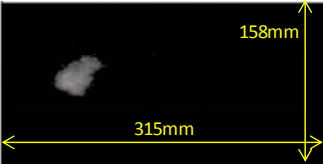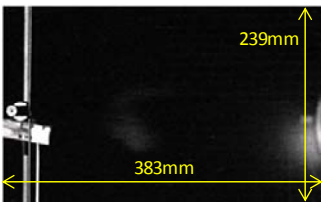
9
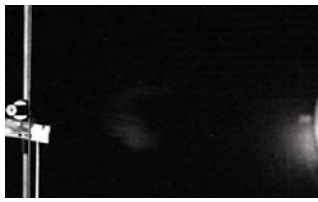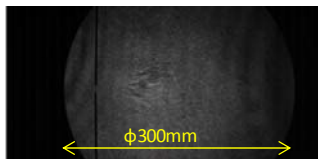
Phase of flame development	Just after ignition	Growth phase of flame	Before flame disappearance
Time from spark (initiation : 0msec)	2msec	10msec	18msec
OH	158mm / 315mm		
H_2O	239mm / 383mm		
Shadowgraph	φ300mm		

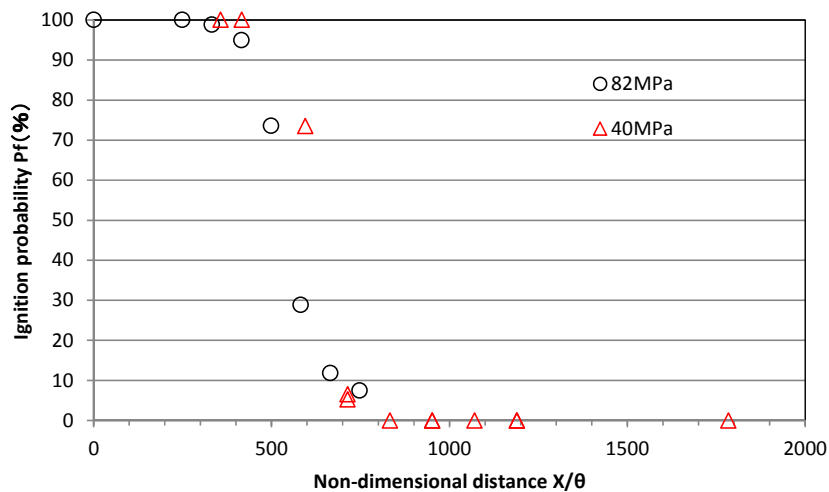Figure 9. Example of recorded images at 600mm from the exit of jet to ignition point

Figure 10. Ignition probability along the jet axis

3.4 Relationship between Ignition and Concentration Fluctuations

The relation among concentration C, occurrence probability P_c of flammable concentration and ignition probability P_f for 82MPa is shown in Fig. 11. In order to study the effect of the different pressures, the concentrations of 60MPa and 40MPa and the occurrence probability of flammable concentration of 40MPa are shown as the experimental data in Fig. 11.

When it is considered that the experiment of 40MPa has the errors due to the outdoor experiment, we may understand all data indicated in Fig. 11 will not depend on the discharge pressure. From Fig. 11, it was found that the averaged concentration C and the occurrence probability of flammable concentration P_c were about 4% and 50%, respectively at the location where the ignition probability P_f is zero. In order to discuss the hydrogen safety, the boundary where ignition probability P_f is zero is a very important factor.

According to the previous study of the hydrogen jet with low exit velocity by Schefer et al. [2], which is in incompressible flow region, their results showed that C and P_c are about 4% and 30%, respectively. It is considered that the difference of P_c from the present study is probably caused by the difference between incompressible jet and compressible jet. It means compressible jet is ignited harder than incompressible one because the velocity in the compressible jet is faster and the jet is stronger than that of incompressible jet.
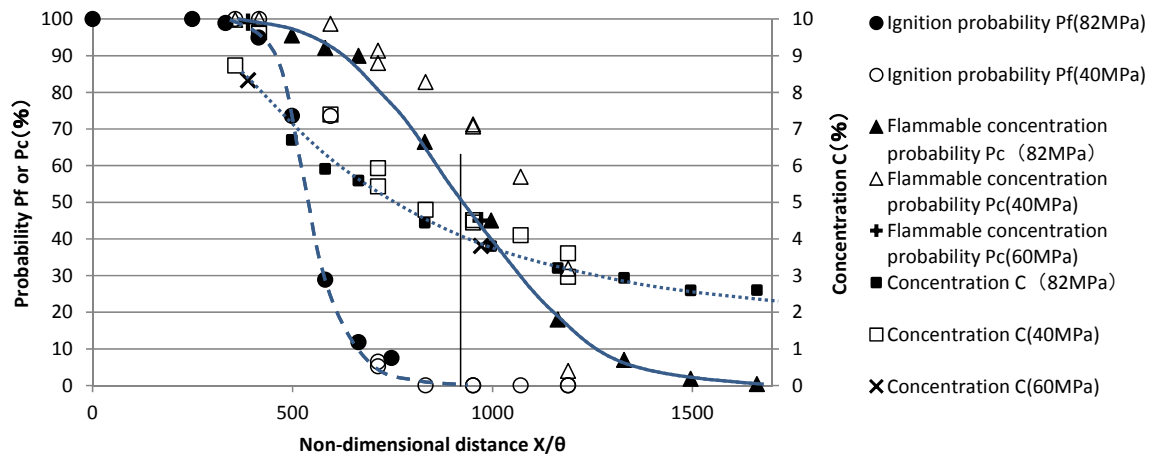

Figure 11. Relationship between Concentration, Ignition and Flammable concentration probabilities

4.0 CONCLUSION

We studied the non-steady behavior of the high-pressurized hydrogen jet with 40 to 82MPa discharge pressure in detail and then discussed about the similarity of flow and dispersion of high-pressurized hydrogen jet to clarify the characteristics of ignitability, normalizing by the representative scales.

Through the above discussion, we tried to obtain the boundary at $P_f=0$ for any high-pressurized hydrogen jet discharged from a diameter of 0.2mm. As results, the boundary where ignition probability P_f is zero would be estimated as follows.

1) From the relation between the concentration C and the distance X expressed by Equation (5), we determine the concentration C(X) at the distance X along the hydrogen jet axis, which is in the jet region without the influence of buoyancy.

2) From the value of the intensity of concentration fluctuation σ_c/C indicated by Equation (7), the standard deviation of concentration fluctuation σ_c is obtained.

3) From the occurrence probability density function P(C) of concentration C expressed by Equations (8) or (9), the occurrence probability of flammable concentration Pc is estimated.

4) By repeating the above procedures from 1) to 3), we can obtain the relationship of the concentration C and the flammable concentration probability P_c against the distance X like Fig. 11.

5) We find out the distance X (the boundary at $P_f=0$) where C and Pc are 4% and 50%, respectively. If the distance X at C=4% and that at Pc=50% are not same, the larger distance may

be better to choose for safety..

We expect the effect of the exit diameter of the hydrogen jet will be also investigated in the future.

5.0 ACKNOWLEDGEMENT

6.0 REFERENCES

1. Kouchi, A., Okabayashi, K., Takeno K., and Chitose K., Proceedings of the Second International Conference on Hydrogen Safety, 11-13 September 2007, San Sebastian (Spain).
2. Schefer, R.W., Evans, G.H., Zhang, J., Ruggles, A.J. and Greif, R., Ignitability Limits for Combustion of Unintended Hydrogen Release: Experimental and Theoretical Results, *International Journal of Hydrogen Energy*, **36**, Issue 3, 2011, pp. 2426-2435.
3. Ruggles, A.J. and Ekoto, I.W., Ignitability and Mixing of Underexpanded Hydrogen Jets, *International Journal of Hydrogen Energy*, **37**, Issue 22, 2012, pp. 17549-17560.
4. Asahi, I., Ninomiya, H. and Sugimoto, S., Remote Sensing of Hydrogen Concentration by Low Power Laser, IEEJ Transactions on Electronics, Information and Systems, 130, No. 7, 2010, pp. 1145-1150.
5. Okabayashi, K., Tagashira, K., Takeno, K., Asahara, M., Hayashi, A.K. and Komori, M., Non-steady Characteristics of Dispersion and Ignitability for High-Pressurized Hydrogen Jet, 54th Symposium (Japanese) on Combustion, Sendai, Sendai International Center (Japan), 23-25 November 2016.
6. Ishigaki, H. and urakami, M., The Properties of a Round Turbulent Buoyant Jet, Technical Report of National Aerospace Laboratory, TR-826, 1984.
7. Okabayashi, K., Nonaka, T., Sakata, N., Takeno, K., Hirashima, H. and Chitose, K., Characteristics of Dispersion for Leakage of High-pressurized Hydrogen Gas, Journal of Japan Society for Safety Engineering, 44, No. 6, 2005, pp. 391-397.
8. Ruggles, A.J. and Ekoto, I.,W., Experimental Investigation of Nozzle Aspect Ratio Effects on Underexpanded Hydrogen Jet Release Characteristics, International Journal of Hydrogen Energy, 39, Issue 35, 2014, pp. 20331-20338.
9. Okabayashi, K., Uchino, T., Tagashira, K., Asahara, M., Hayashi, A.K. and Komori, M., Characteristics of Dispersion and Ignitability for 82MPa High-pressurized Hydrogen Jet discharged from a Pinhole, Proceedings of the 2016 year's Autumn Meeting of Japan Explosive Society, 10-11 November 2016, Nagasaki (Japan), pp.119-122
10. Sato, K., Behavior of a Jet Discharged at High Pressure, Journal of Japan Society for Safety Engineering, 23, No. 2, 1984, pp. 88-92.
11. Yee, E., Wilson, D.J. and Zelt, B.W., Probability Distributions of Concentration Fluctuations of a Weakly Diffusive Passive Plume in a Turbulent Boundary Layer, Boundary-Layer Meteorology, 64, 1993, pp. 321-354.
12. Hanna, S.R., The Exponential Probability Density Function and Concentration Fluctuations in Smoke plume, Boundary-Layer Meteorology, 29, 1984, pp. 361-375.
13. Hanna, S.R. and Insley, E.M., Time Series Analyses of Concentration and Wind Fluctuations, Boundary-Layer Meteorology, 47, 1989, pp. 131-147.
14. Pasquill, F., Atmospheric Diffusion (2nd Edition), Ellis Horwood Ltd., 1974, p. 61.